Chemical Science

Accepted Manuscript

This article can be cited before page numbers have been issued, to do this please use: Y. Wang, K. Li, Y. Yang, R. Tian and C. Lu, *Chem. Sci.*, 2026, DOI: 10.1039/D5SC09282E.

ROYAL SOCIETY OF CHEMISTRY

rsc.li/chemical-science

View Article Online
DOI: 10.1039/D5SC09282E

ARTICLE

Break the paradox: simultaneous recovery of phosphorescence and mechanics for polymeric films

Received 00th January 20xx,
Accepted 00th January 20xx

DOI: 10.1039/x0xx00000x

Yan Wang,†[a] Kaitao Li,†[ac] Yongpeng Yang,†[b] Rui Tian,*[ac] and Chao Lu*[abc]

Polymeric films with self-healable room temperature phosphorescence (RTP) and mechanical performances are eagerly needed in the wearable and electronic devices. However, it remains a great challenge to simultaneously recover phosphorescence and mechanical properties, due to the improper interaction to quench phosphorescence and inherent conflict between the chain rigidity and flexibility in polymeric films. Herein, we have proposed a chromophore binder between polymer matrix to fabricate RTP films with simultaneous recovery of phosphorescence and mechanics. Cross-linking covalent network has been established, restricting molecular motion of chromophore binders to achieve bright deep blue phosphorescence emissions. Meanwhile, the films exhibited processability, flexibility, stretchability, and self-healing ability. Note that both phosphorescent and mechanical properties could be recovered with efficiency of more than 90% for the films healed in water under room temperature. Theoretical simulation showed that such a decent self-healing capacity could be ascribed to the relatively low energy to form and re-form covalent cross-linkage between chromophore binders and polymer matrix. Accordingly, we have realized an assemble-reassemble process for multi-emission phosphorescence by healing film fragments using different chromophores with boronic acid groups. It is anticipated that such a facile and universal strategy through covalent cross-linkage could provide possibilities for the design of multi-functional optical materials with expanded application fields.

Introduction

Room temperature phosphorescence (RTP) films with decent mechanical performances have shown great promise in flexible optical communication,[1-3] displays, and e-skin.[4-6] These applications impose restrict demands for mechanical deformation with sustainable phosphorescence emissions. Unfortunately, overloaded mechanical forces may induce structural damage and functional degradation for these RTP films, to ultimately lead to the decayed lifetime and encryption data loss.[7-9] Currently, self-healing strategy has been proposed to restore structure and functionalities,[10-12] requiring high chain mobility to diffuse along the polymer interfaces for healing process. However, it is well known that flexible and mobile chains are detrimental to depress the non-radiative transition for phosphorescence emissions, which may lead to the compromise of phosphorescence loss in the self-healed films. Moreover, the improper healing condition would also quench the triplet exitons to recover phosphorescence, even the mechanical properties could be recovered. Therefore, great efforts should be paid to solve the conflict between the rigidity and flexibility of polymers for self-healable polymeric films to recover both phosphorescence and mechanics.

Incorporation of a small-molecular binder between polymer matrix has been proposed as a facile self-healing strategy.[13,14] Specifically, the interaction between the binder and polymer matrix is vital to recover the functionalities of the polymeric films by changing the functional groups of the binder.[15] Currently, dynamic covalent or non-covalent interactions have been exploited to realize the self-healing strategies, such as disulfide bonds,[16] imine bonds,[17] Diels–Alder bonds, and borate ester bonds.[18,19] However, most of these covalent bonds are initiated by the external energy. For example, imine and boron ester bonds, with the bonding energy of 600 and ~500 kJ/mol,[20] require heat energy to trigger the reaction for self-healing. Polymers with disulfide bonds could be self-healed under 70 °C,[21] and Diels–Alder bonds could be formed under 80 °C.[22] Notably, most phosphorescent chromophores are unstable under thermal treatment, and the heat-intensified non-radiative transition leads to the decayed persistent afterglow and hindered healing efficiency.[23,24] Alternatively, hydrogen bond with low binding energy could be adopted to heal the polymers under room temperature. Disappointedly, the uptake of water is generally occurred in the presence of hydrogen bonds, leading to the reduced stiffness and quenched RTP properties of the polymeric films.[25,26] Therefore, it remains a current challenge to design a facile strategy to achieve high self-

[a] State Key Laboratory of Chemical Resource Engineering, Beijing University of Chemical Technology, Beijing 100029, China
[b] Pingyuan Laboratory, College of Chemistry, Zhengzhou University, Zhengzhou, 450001, China
[c] Quzhou Institute for Innovation in Resource Chemical Engineering, Quzhou, 324000, China
E-mail: tianrui@mail.buct.edu.cn (R. Tian), luchao@mail.buct.edu.cn (C. Lu)
† Authors with equal contribution to the work.
Electronic Supplementary Information (ESI) available. See DOI: 10.1039/x0xx00000x

View Article Online
DOI: 10.1039/D5SC09282E

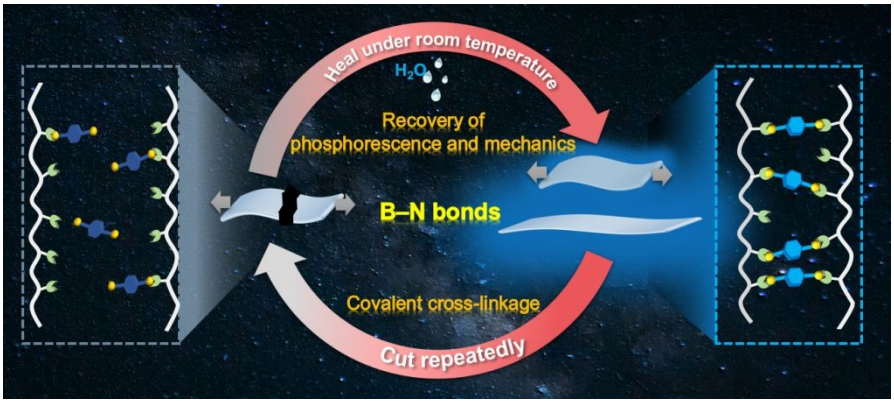

Scheme 1 Schematic diagram to prepare a self-healing material with simultaneous recovery of phosphorescent and mechanical performances through B-N covalent bonds.

healing efficiency under room temperature without phosphorescence decay.

B–N bonds could be formed under mild condition through click reaction with the binding energy of around 100 kJ/mol.[27] In this work, we have employed B–N covalent bonds to prepare a self-healable RTP material, based on polyacrylamide (PAM) with abundant amino groups and chromophore binders with boronic acid groups (Scheme 1). Bright deep blue phosphorescence was acquired due to the restricted molecular motion and regulated molecular arrangement of chromophore binders. Meanwhile, the as-prepared polymeric RTP films exhibited elongation rate of 530% with uniformly-distributed phosphorescence upon stretching. It is noteworthy that not only mechanical performances, but also RTP of the films, could be simultaneously recovered for more than 90% of pristine values upon the self-healing in water at room temperature. Such a cutting-healing cycle could be repeated consecutively through the broken and re-formation of covalent bonds. We have confirmed the advantages of facile B–N covalent cross-linkage in promoting RTP and self-healing performances through the condensation energy calculation by density-functional theory simulation. Furthermore, the recycle ability of these self-healing RTP films was validated by assembling-reassembling different pieces of cross-linked films. As expected, multi-phosphorescence emissions could be acquired by self-healing, and the healed sites exhibited decent phosphorescence and mechanical performances even under folding, stretching and rotating states. Therefore, the simultaneous recovery of deep blue RTP and mechanical properties could be observed for polymeric RTP films, demonstrating the advantages of covalent cross-linkage between chromophore binders and polymer matrices. It is anticipated that the established covalent cross-linking strategy could open a new avenue for the design of practical optical devices with promoted durability, safety, and the security levels of the stored confidential information.

Results and discussion

RTP and mechanical properties of *x*% BDBA-PAM films

We have chosen 1,4-benzenediboronic acid (BDBA), which possess two boronic acid groups attached at the terminals of phenyl group, as the binders to construct composite films. Green phosphorescence emission centered at 500 nm could be observed for BDBA powder under excitation of 280 nm (Fig. S1 and S2). In comparison, the low-temperature phosphorescence spectra of BDBA aqueous solution (10^{-6} mol/L) recorded in the liquid nitrogen showed dark blue emission around 410 nm (Fig. S3). These two different emission centers at 500 and 410 nm suggested the aggregated and isolated states of BDBA, respectively.[28] Accordingly, BDBA molecule with boronic acid groups was selected as binder to cross-link PAM with amino groups through B–N bonds. BDBA-PAM composite films were successfully prepared, with the uniformly distributed boron, carbon, oxygen, and nitrogen elements throughout the films as observed from scanning electron microscopy and energy dispersive spectrometry (Fig. S4). All the *x*% BDBA-PAM films showed deep blue phosphorescence emissions at 410 nm under the excitation wavelength of 280 nm, while the pure PAM showed no phosphorescence emission (Fig. 1a). Such a deep blue phosphorescence could be ascribed to the depressed self-condensation and isolated states of BDBA molecules after reaction with PAM through the covalent bonds. The RTP emissions of the *x*% BDBA-PAM films were promoted with the increased BDBA contents (*x*%) from 0 to 1.0%, followed by a decrease with the excess BDBA to 1.5% (Fig. 1a, inset). The decayed RTP performances for 1.5% BDBA-PAM could be ascribed to the fact that the amino groups in the PAM were not sufficient to localize all the BDBA molecules through the B–N bond, and some free BDBA molecules dissipated energy through the molecular motion. Similar tendency could also be observed for the lifetimes of *x*% BDBA-PAM films: the lifetimes at 410 nm showed an increase to 160 ms for 1.0% BDBA-PAM film and then a decrease afterwards (Fig. 1b). Temperature-dependent lifetimes validated the nature of phosphorescence for BDBA-PAM composite films (Fig. S5). These phenomena could be validated by the photographs of the *x*% BDBA-PAM films using UV-LEDs as a light source. Deep blue afterglows around 3 s could be traced by the naked eyes for *x*% BDBA-PAM films when the UV lamp was switched off (Fig. 1c), and 1.0% BDBA-PAM film showed the strongest phosphorescence intensity and the longest lifetime. In comparison, no phosphorescence could be observed for the pure PAM upon

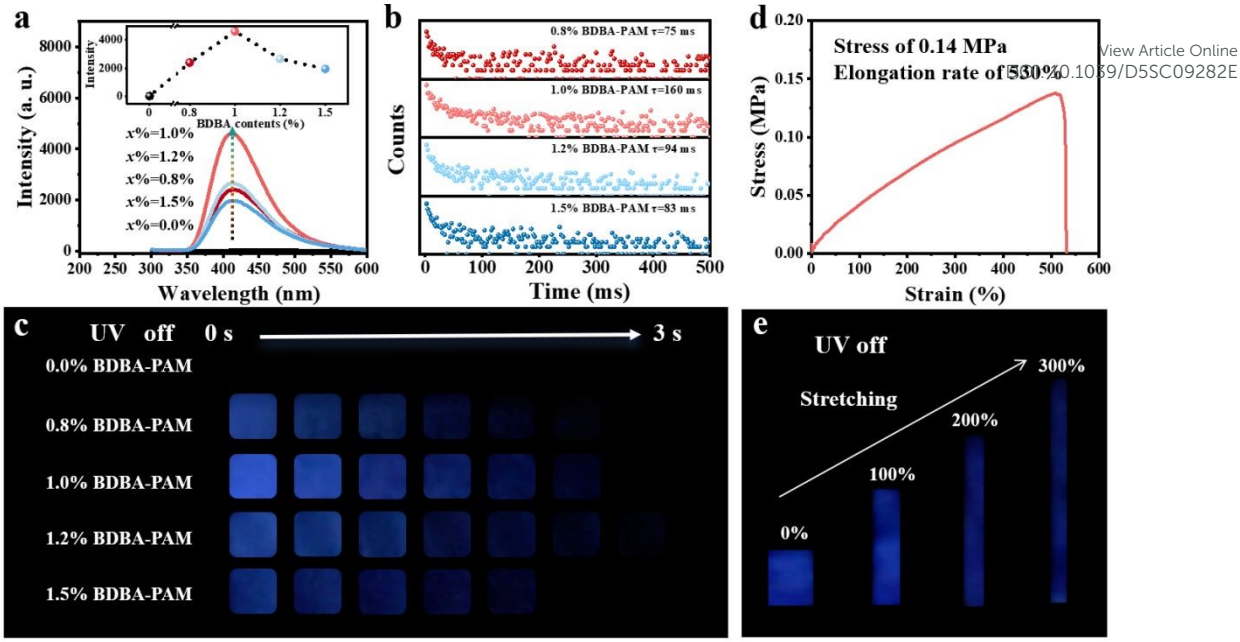

Fig. 1 RTP behaviors and mechanical performances of *x*% BDBA-PAM films. (a) Phosphorescent emission spectra (the inset showed the variations of RTP intensities); (b) Phosphorescence lifetimes and (c) photographs of *x*% BDBA-PAM films; (d) Mechanical property curve of 1% BDBA-PAM composite film and (e) phosphorescence photos of BDBA-PAM films under different stretching rates.

irradiation. These results suggested the promoted phosphorescent behaviors of BDBA molecules, which could be ascribed to the increased rigidity of the composite films based on the covalent network between BDBA and PAM.

The mechanical properties of BDBA-PAM composite films were studied by tensile testing measurements. The stress-strain curve showed that the stress of 1.0% BDBA-PAM composite film was 0.14 MPa, and its elongation rate could reach 530% (Fig. 1d). In comparison, the elongation rate of pristine PAM was only 180% (Fig. S6). This comparison demonstrated the good flexibility of the cross-linked BDBA-PAM film. To investigate the RTP performances of the film under stretching, the 1.0 % BDBA-PAM film was stretched to 0, 100, 200 and 300% of the original lengths, and the phosphorescence photos were captured after turning off UV lamp. Uniform and strong deep blue afterglows could be observed throughout the 1.0 % BDBA-PAM film with the stretching rate from 0% to 300% (Fig. 1e), which could be ascribed to the uniform distribution of BDBA as binders to cross-link PAM in the composite films. These results demonstrated the stable and decent RTP performances for BDBA-PAM composite films under different elongation rates.

Self-healing performances of *x*% BDBA-PAM films

Self-healing ability of the BDBA-PAM composite film was studied. In a typical healing experiment, the film was cut into two pieces. Water, an environmentally friendly reagent, was added dropwise to the fracture between these two pieces for healing. Upon the addition of the healing agent (water) under room temperature, the motions of BDBA and PAM molecules were initiated at the fracture, leading to the reconstruction of B–N covalent bonds at the interfaces. The self-healing process of BDBA-PAM composite film were proceeded under room temperature. After treatment for 5 min, the two pieces of the BDBA-PAM films were self-healed and could be picked up as a body by a tweezer (Fig. S7a). In contrast, the pure PAM film failed to be healed under the same condition (Fig. S7b), suggesting the key role of binders with boronic acid groups to achieve self-healing ability for BDBA-PAM composite films. With the prolonged treatment time, more B–N covalent bonds were reconstructed to heal the BDBA-PAM composite film. The BDBA-PAM composite films were recovered to the original shape after treatment for 0.5 h, and no cracks could be observed from the photos taken under daylight (Fig. 2a, inset, top). The fracture evolution in BDBA-PAM composite film during the healing process could be identified by the phosphorescence after turning off the UV light. Faint phosphorescence emissions could be observed near the fracture after self-healing for 0.5 h, and the blue afterglows recovered gradually with the prolonged time to 3 h. Bright and strong phosphorescence could be observed throughout the film after self-healing for 14 h (Fig. 2a, inset, top). The self-healing ability of the BDBA-PAM composite film was further observed using an electron microscope: the cracks grew smaller with the healing time prolonged to 3 h and healed after 14 h (Fig. 2a, inset, bottom). These results demonstrated the recovered completeness and phosphorescence of the BDBA-PAM composite films after self-healing process. In comparison, we have prepared referenced film samples employing PVA as polymer matrix. The hydroxyl groups in PVA could react with BDBA molecules to form B–O covalent bonds. However, the cut pieces of BDBA-PVA film could not be healed under the same cutting-healing process, and no phosphorescence emissions could be observed for these films (Fig. S8). These results demonstrated the advantages of B–N covalent bonds than B–O bonds to prepare cross-linked

View Article Online
DOI: 10.1039/D5SC09282E

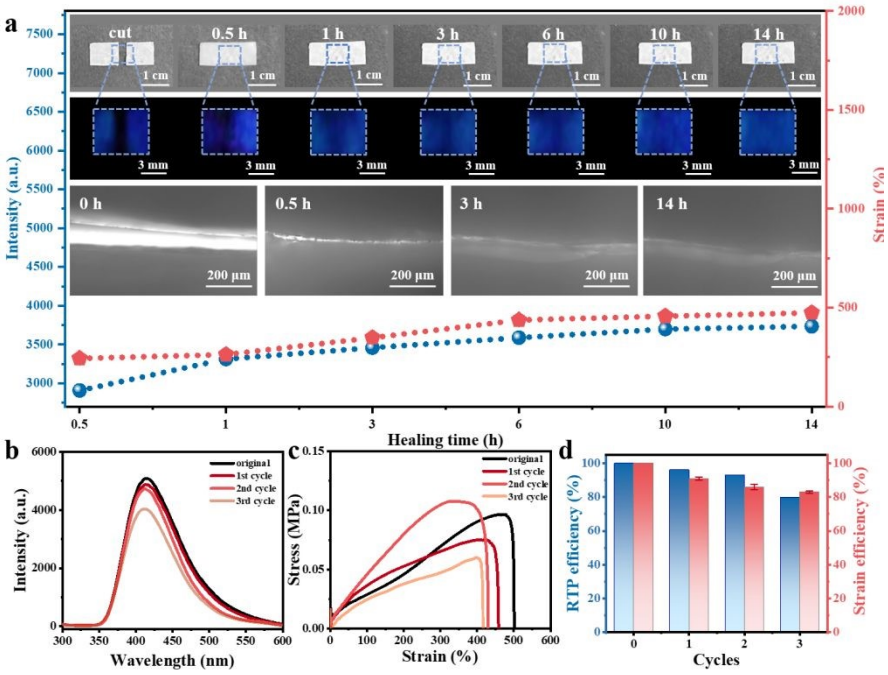

Fig. 2 RTP and mechanical performances of 1% BDBA-PAM film during room temperature self-healing process by water as healing reagent. (a) Variations of phosphorescent and mechanical properties for BDBA-PAM films at different self-healing time, the inset showed the photos under daylight, after the UV light off and electron microscopic images for BDBA-PAM films during the self-healing process; (b) Phosphorescence spectra; (c) stress-strain measurements and (d) self-healing efficiencies of BDBA-PAM films at different cutting-healing cycles.

BDBA-PAM composite films which could be self-healed under room temperature using water as healing agent.

Both RTP and mechanical properties were taken as key parameters to evaluate the self-healing efficiencies of the BDBA-PAM composite films. The phosphorescence intensity at the fracture recovered to 71% after healing for 0.5 h (Fig. S9a), followed by the continuous increase to 92% at 14 h (Fig. 2a and Table S1). Moreover, the mechanical properties of the BDBA-PAM composite films also showed an increasing trend: the elongation rate reached 478% after healing for 14 h (Fig. S9b), which is more than 90% of the pristine film (Table S1). This cutting-healing process was then repeated for BDBA-PAM film under room temperature taking water as healing reagent. Satisfactorily, the phosphorescence emissions of the BDBA-PAM film could recover to 90% of the original intensities after three consecutive cutting-healing cycles (Fig. 2b and Table S2), and healing efficiency of the mechanical properties could reach 83% (Fig. 2c and 2d). Therefore, efficient self-healing performances could be realized for BDBA-PAM films, with both recovered phosphorescent and mechanical behaviors.

Structural characterization of *x*% BDBA-PAM films during self-healing process

In order to figure out the interaction between BDBA and PAM, Fourier transform infrared spectroscopy (FT-IR) was carried out for the BDBA-PAM composite films.[29,30] The absorption peaks of the O–H bonds in the range of 3200 – 3400 cm^{-1} and characteristic peak of B–O bond near 1340 cm^{-1} could be observed for BDBA (Fig. 3a). PAM showed characteristic peaks around 3445 cm^{-1}, attributed to the stretching vibration of NH_2.[31] This characteristic peak of PAM shifted to the lower wavenumber after reaction with BDBA, indicating the decreased contents of amino groups due to the formation of B–N covalent cross-linking. Notably, new peaks at 1398 cm^{-1} and 720 cm^{-1} were identified in the BDBA-PAM composite film, ascribed to the stretching vibration and bending vibration of the B–N bonds.[32] The appearance of these peaks verified the successful covalent cross-linking between BDBA and PAM in the composite film. Notably, these peaks ascribed to the B–N bond could also be identified for the BDBA-PAM film healed in water, suggesting the successful reconstruction of B–N bonds in the film after healing process.

X-ray diffraction (XRD) measurements were further implemented for the BDBA-PAM films. Characteristic diffraction peaks of PAM appeared at 31.9° and 45.4°, indicating the crystallization of PAM (Fig. 3b). After reaction with BDBA, the characteristic peaks at 28.5° of BDBA could be identified in the BDBA-PAM composite films. In addition, the crystalline peaks at 31.9° and 45.4°of PAM increased significantly from 11.59% to 30.26%, suggesting the improved molecular chain regularity and promoted crystallinity of PAM in the BDBA-PAM composite films. This phenomenon could be ascribed to the modified molecular arrangement of PAM after the covalent cross-linking reaction with BDBA binder.[33] After the cutting-healing process, the PAM in BDBA-PAM composite showed the similar peak shape with crystallinity of 34.22%, suggesting that PAM remained the same structure after the break and reconstruction of B–N bonds.

UV-Vis absorption spectra of BDBA, PAM and BDBA-PAM composites were further studied. Characteristic n-π* transition with absorption peaks at 250–400 nm[34] could be identified, which was significantly enhanced for the BDBA-PAM composite

View Article Online
DOI: 10.1039/D5SC09282E

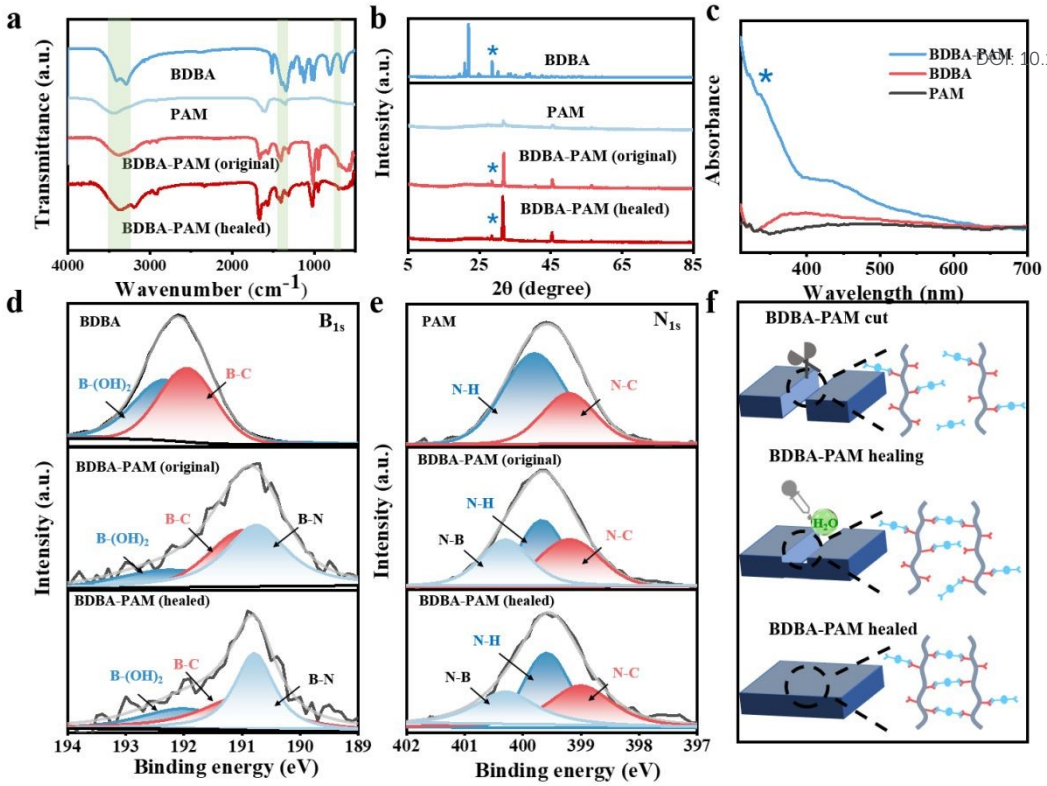

Fig. 3 Structural studies for x% BDBA-PAM composite films before and after self-healing process. (a) FT-IR spectra; (b) XRD patterns; (c) UV-Vis spectra; (d) B 1s and (e) N 1s spectra for BDBA, PAM, BDBA-PAM films before and after healing process; (f) Mechanism diagram of healing process of BDBA-PAM based on B-N covalent cross-linking.

film than that of BDBA (Fig. 3c). This result demonstrated that the N atoms in PAM could provide lone-pair electrons towards the benzene unit through the covalent B–N and facilitate the n-π* transition for phosphorescence in BDBA-PAM.

The changes in chemical bonding in the composite films were further investigated using X-ray photoelectron spectroscopy (XPS).[35,36] The B 1s spectrum of BDBA at 192.08 eV could be split into peaks of B–$(OH)_2$ (192.30 eV) and B–C (191.90 eV).[37] The B 1s peak shifted to 190.80 eV in BDBA-PAM composite films (Fig. 3d), with the appearance of new peaks for B–N (190.70 eV). Note that the content of B–$(OH)_2$ decreased from 50.0% in BDBA to 16.2% in the BDBA-PAM composite films, with the accumulated content of B–N up to 38.6% (Table S3). After the healing process, the content of B–N bonds was about 37.1%, suggesting the successful reconstruction of BDBA-PAM composite films. For N 1s spectra, N–H (399.80 eV) and N–C (399.19 eV) bimodal peaks could be observed in PAM,[38] and a new peak ascribed to N–B could be observed at 400.20 eV in the BDBA-PAM composite film (Fig. 3e). The N–H bonds decreased from 66.7% in PAM to 33.5% in BDBA-PAM composite, associated with the increased content of N–B for 33.3% (Table S4). These results indicated that the covalent interaction has consumed NH_2 in PAM, and N–B bonds were formed in the composite films. After the healing process, we can identify the reconstruction of N–B bonds by the almost unchanged contents before and after healing process. Similar changes could also be observed in the C 1s spectra for BDBA, PAM and BDBA-PAM composite films (Fig. S10 and Table S5), according to the C–C/C=C bonds from C 1s spectrum at 284.8 eV.[39] These results demonstrated the formation of covalent cross-linking between BDBA and PAM in the composite films, enhancing the network rigidity and promoting RTP/mechanical properties. The dynamic reversibility of these B–N covalent bonds endowed the composite materials with self-healing performances: broken upon cutting process and restored under the healing in water (Fig. 3f).

Theoretical simulation of phosphorescence and self-healing mechanisms for the composites

We have explored time-dependent density-functional theory (TD-DFT) calculations to explain the decent RTP and self-healing mechanism for the composites. For the RTP behavior studies, the T_1 energy level of singular BDBA molecule was calculated as 2.98 eV, corresponding to the phosphorescence emission at 415 nm (Fig. 4a). However, the BDBA molecules are prone to aggregate and self-condense, leading to a decrease in the T_1 energy level and a red shift in the phosphorescence emission (Fig. 4b). The energy of the T_1 energy level decreased to 2.43 eV with the number of self-condensed molecules increased to 9, and the calculated theoretical phosphorescence emission wavelength red shifted to 511 nm (Fig. 4c). These results indicated that the dark blue phosphorescence at 410 nm of BDBA-PAM could be attributed to the mono-dispersed state of BDBA isolated by the polymer matrix.

The geometries of BDBA and BDBA-PAM were further explored. We have studied the ability of boronic acid groups in

View Article Online
DOI: 10.1039/D5SC09282E

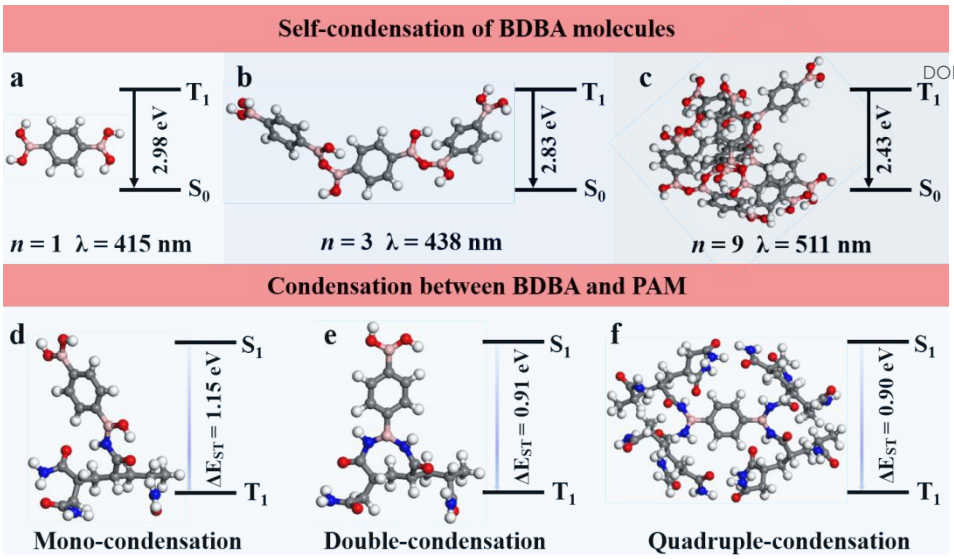

Fig. 4 Structural models and the energy level diagrams between the triple excited states and ground states of (a-c) self-condensation of BDBA and (d-f) condensation between BDBA and PAM.

BDBA to condense with amide groups in PAM by calculating the free energy of condensation between BDBA and PAM. It is suggested that one boric acid group favored the condensation with one amide group in a PAM chain with a free energy of 0.44 eV (Fig. 4d), rather than condensation with two neighboring amide groups in a PAM chain with the energy of 0.75 eV for per condensation (Fig. 4e). Accordingly, two boronic acid groups in BDBA molecule were apt to condense with four different PAM chains to form a cross-linking network (Fig. 4f). The energy required for hydrolysis of B–N bonds from cross-linked films was calculated as –0.44 eV per condensation, which was apt to be realized. Such a result demonstrated the decent self-healing capacities of the BDBA-PAM composite films. In comparison, poly(vinyl alcohol) (PVA) with hydroxyl groups were employed to react with boric acid in BDBA through B–O bonds. Differently, the boronic acid in BDBA were apt to condense with two neighboring hydroxyl groups in one PVA chain with a free energy of 0.11 eV for per condensation, instead of the condensation with a single hydroxyl group in PVA chain with a free energy of 0.39 eV (Fig. S11). The energy required for hydrolysis in BDBA-PVA was estimated as 0.28 eV, explaining the failure in the self-healing.

Furthermore, BDBA-PVA showed an energy level difference of the leap energy as 1.19 eV, which was larger than the energy level difference of 0.90 eV for BDBA-PAM. The smaller of ΔE_{ST} for BDBA-PAM suggested the easier of intersystem crossing process and stronger RTP,[40] in comparison with BDBA-PVA. Accordingly, BDBA-PAM with the B–N cross-linkage featured decent RTP and self-healing performances.

Versatility studies for self-healing RTP films

We have further employed two other boronic acid-derived binders to investigate the versatility of the B–N covalent bonding to prepare cross-linked self-healing composites with simultaneously recovery of RTP and mechanical properties. In brief, 4,4'-biphenyldiboronic acid (BPBA), and 1-naphthylboronic acid (1NB) were used to react with PAM to prepare BPBA-PAM and 1NB-PAM composite films. Bright phosphorescence emissions could be observed after turning off UV light: cyan emission of 7 s for BPBA-PAM and green afterglow of 8 s for 1NB-PAM (Fig. 5a). In contrast, the phosphorescent afterglow of BPBA and 1NB powder were hardly to observe by the naked eyes when the UV lamp was switched off (Fig. S12). The phosphorescence lifetime of 0.5 ms for BPBA powder was promoted to 710 ms for BPBA-PAM composite, while the 1NB-PAM showed longer lifetime of 695 ms than 0.2 ms for the 1NB powder (Fig. S13). Moreover, it could be observed that phosphorescence emission of BPBA blue-shifted from 540 nm in powder to 480 nm in the covalently cross-linked BPBA-PAM composite film (Fig. 5b). Differently, the phosphorescence of 1NB were red-shifted from 410 nm in powder to 490 nm and 520 nm for 1NB-PAM (Fig. 5c). These phenomena could be ascribed to the different molecular structures of boronic acid-modified chromophores. BPBA molecules with boronic acid groups attached at two ends of biphenyl are apt to form a cross-linked structure with PAM, so that the BPBA could be well localized by the PAM network. In contrast, 1NB with only one boronic acid could not be efficiently immobilized by PAM, leading to the unavoidable molecular aggregation.

The mechanical and RTP properties under stretching for BPBA-PAM and 1NB-PAM composite films were also studied. Phosphorescent photographs were taken by stretching the composite films to 0, 100, 200 and 300% of the original length, and bright cyan and green afterglows could be observed throughout BPBA-PAM and 1NB-PAM films (Fig. 5d and 5e).

Self-healing capacities of these composite films were then explored under the same conditions using water as healing agent. Adding water along the fracture of the films, the cut pieces could be healed into one piece at room temperature within a few minutes. The phosphorescent intensities of BPBA-PAM recovered to 88% of the original values after the healing process (Fig. 5f), while the phosphorescence recovery of 1NB-PAM film could only reach 71% (Fig. 5g). Meanwhile, healing

View Article Online
DOI: 10.1039/D5SC09282E

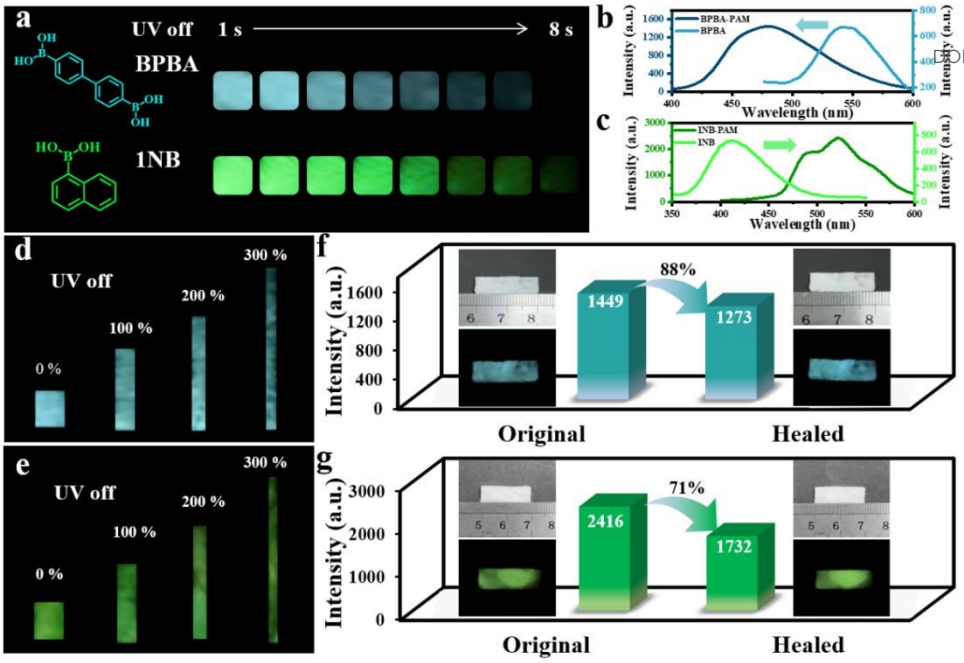

Fig. 5 Phosphorescent and self-healing behaviors of BPBA-PAM and 1NB-PAM composite films. (a) Photos of BPBA-PAM and 1NB-PAM composite films taken after UV light was off; Phosphorescence spectra of (b) BPBA powder (light blue), BPBA-PAM films (blue), and (c) 1NB powder (light green), 1NB-PAM films (green); Phosphorescence photos of (d) BPBA-PAM and (e) 1NB-PAM composite films under different stretching rates; Phosphorescence recovery efficiencies of (f) BPBA-PAM and (g) 1NB-PAM composite films after healing process (the inset showed photos of self-healing process under daylight and after UV light was off).

efficiency of 90% and 75% for the mechanical properties could be achieved for BPBA-PAM and 1NB-PAM composite films, respectively (Fig. S14). For a comprehensive comparison, BDBA-PAM and BPBA-PAM possessed higher healing efficiencies in both RTP and mechanical properties than that of 1NB-PAM (Fig. S15). Such a result could be ascribed to the higher possibilities of BDBA and BPBA, with two boronic acid groups at both ends of benzene rings, to covalently bind to PAM to form a cross-linked network. Therefore, we can demonstrate the universality of the dynamic B–N bond to prepare composite films with room temperature self-healing and phosphorescence performances.

Applications of self-healing RTP films

Anti-counterfeiting and recycling applications of B–N based composite films were studied. As validated from the CIE coordinates, varied phosphorescence colors from blue emissive BDBA-PAM (0.156, 0.083), cyan colored BPBA-PAM (0.156, 0.274) to greenish 1NB-PAM (0.218, 0.544) were identified and

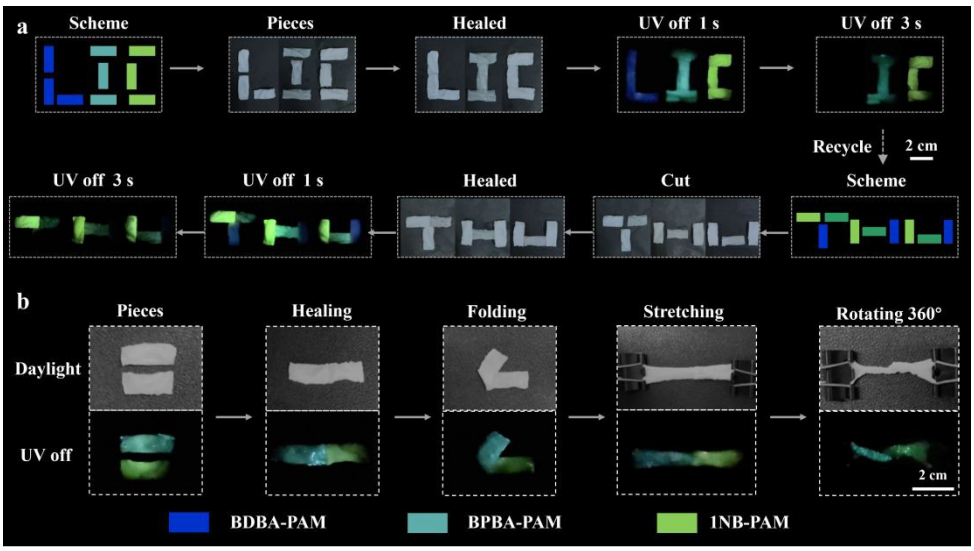

Fig. 6 Recycle and anti-counterfeiting applications for BDBA-PAM, BPBA-PAM and 1NB-PAM composite films: (a) cut and assembled to the different letters and their afterglows for anti-counterfeiting, and (b) folding, stretching and rotating behaviors of the healed composite films.

View Article Online
DOI: 10.1039/D5SC08282B

used for anti-counterfeiting (Fig. S16). First, BDBA-PAM, BPBA-PAM and 1NB-PAM composite films were cut into rectangles with the size of 2 × 1 cm^2. The BDBA-PAM fragments were put together to assemble letter "L", followed by the addition of water for a self-healing process (Fig. 6a). Similarly, the BPBA-PAM fragments were assembled to letter "I", and a letter "C" was assembled by the 1NB-PAM pieces. After healing in water for 5 min, morphological completeness could be recovered, and a phosphorescence "LIC" pattern could be observed after the ultraviolet lamp was turned off. The assembled letter "L", "I" and "C" showed dark blue, cyan and green phosphorescence emissions, respectively. A colored "LIC" pattern was changed to "IC" after 3 s with the disappearance of dark blue BDBA-PAM. In addition, the composed pattern with assembled BDBA-PAM, BPBA-PAM and 1NB-PAM fragments was cut and healed again for recycling and reassembling process. Five min later, "THU" pattern with integrated blue, cyan and green phosphorescence emissions was re-organized upon healing by water. The composite films retained their RTP properties after recycling process. After a delay of 3 s, an irregular pattern with cyan and green afterglows was displayed, demonstrating the potential applications for multi-stage encryption.

In addition, we have also explored the flexibility and deformation ability of the healed films. Pieces of BPBA-PAM and 1NB-PAM composite films with rectangular shape were organized for the tests. These films were healed with water and assembled into rectangles with cyan (left) and green (right) emissions (Fig. 6b). The assembled composite films can be folded, stretched and rotated for 360° without breaking at the healed site. It is satisfactory that the assembled composite films showed decent mechanical properties, and bright dual-color phosphorescent afterglow can be observed throughout the whole film. These results highlighted the advantages of stretchable, self-healable and phosphorescent performances for the composite films based on the dynamic B–N covalent bonds, which showed great potential to achieve encryption behaviors with long lifetime and lossless readout capabilities.

Conclusions

In summary, we have proposed B–N bonds between chromophore binders and polymer matrix to establish a covalent cross-linked network for room-temperature self-healing composite films. The B–N bonds could construct a covalent network to increase the rigidity of the composite films for boosted RTP performances, and the composite films showed decent mechanical properties with uniform phosphorescence emissions under stretching. More importantly, both phosphorescence and mechanical properties could be simultaneously recovered for such a covalently bonded film after several cutting-healing cycles. The proposed strategy is applicable to different binders with boronic acid groups, and the prepared composite films could be assembled and reassembled into a complete body after self-healing process in water. These results highlighted the power of the dynamic covalent bonds on the structural optimization and performance promotion for functional polymeric films. The proposed strategy showed decent versatility and potential ability in anti-counterfeiting and information storage. It is expected that the proposed strategy could be further extended for the design and preparation of multi-functional materials.

Author contributions

C. L., and R. T. conceived the experiments. Y. W. carried out the experiments. Y. P. Y. conducted theoretical calculations. Y. W., K. T. L., Y. P. Y., R. T., and C. L. contributed to data analysis and writing of this manuscript.

Y. W., K. T. L., and Y. P. Y contributed equally to this work.

Conflicts of interest

There are no conflicts to declare.

Acknowledgements

This work was supported by the National Natural Science Foundation of China (22374008, 22534007 and U22A20397), and the Key Research and Development Program of Henan province (251111321000).

Notes and references

1 D. X. Ma, Z. Q. Li, K. Tang, Z. L. Gong, J. Y. Shao and Y. W. Zhong, *Nat. Commun.*, 2024, **15**, 4402.
2 M. Q. Dai, Z. H. Qi and D. P. Yan, *Angew. Chem. Int. Ed*., 2025, **64**, e202420139.
3 F. Nie and D. P. Yan, *Acc. Chem. Res.*, 2025, **58**, 3010.
4 Y. F. Yang, Y. H. L, Y. T. Zheng, J. A. Li, S. Y. Wu, H. Q. Zhang, T. P. Huang, S. L. Luo, C. Liu, G. Shi, F. Q. Sun, Z. G. Chi and B. J. Xu, *Angew. Chem. Int*. Ed., 2022, **61**, e202201820.
5 H. Gao and X. Ma, *Aggregate*, 2021, **2**, e38.
6 F. Nie and D. P. Yan, *Sci. China Mater.*, 2024, **67**, 3531.
7 Y. C. Liu, T. Chen, Z. Jin, M. Li, D. Zhang, L. Duan, Z. Zhao and C. Wang, *Nat. Commun.*, 2022, **13**, 1338.
8 B. Yang and W. Yuan, *ACS Appl. Mater. Interfaces*, 2019, **11**, 16765-16775.
9 C. H. An, F. M. Nie, R. J. Zhang, X. L. Ma, D. H. Wu, Y. Sun, X. D. Hu, D. Sun, L. Pan and J. Liu, *Adv. Funct. Mater.*, 2021, **31**, 2100136.
10 G. J. Liang, Z. X. Liu, F. N. Mo, Z. J. Tang, H. F. Li, Z. F. Wang, V. Sarangi, A. Pramanick, J. Fan and C. Y. Zhi, *Light-Sci Appl.*, 2018, **7**, 102.
11 P. Hu, S. Zhou, Y. Wang, J. H. Xu, S. Zhang and J. J. Fu, *Chem. Eng. J.*, 2022, **431**, 133728.
12 Y. Wang, M. Zheng, X. Wang, S. H. Li and J. Q. Sun, *ACS Appl. Mater. Interfaces*, 2018, **10**, 30716-30722.
13 Q. Song, Z. L. Liu, J. W. Li, Y. B. Sun, Y. Q. Ge and X. Y. Dai, *Adv. Mater.*, 2024, **36**, 2409983.
14 R. L. Guo, W. N. Qi, H. Y. Liu, D. X. Li, G. X. Chen, Q. F. Li and Z. Zhou, *Chem. Eng. J.*, 2024, **485**, 149850.
15 S. Zheng, S. Y. Zhong, X. M. Liu and S. L. Sun, *Chem. Eng. J.*, 2025, **509**, 161485.
16 X. Zhang, F. H. Dong, M. M. Yu, X. Xu, H. Liu and H. Q. Lu, *Chem. Eng. J.*, 2025, **507**, 160302.

View Article Online
DOI: 10.1039/D5SC09282E

17 Q. Y. Fan, Y. T. Tang, H. N. Sun, D. K. Guo, J. W. Ma and J. B. Guo, *Adv. Mater.*, 2024, **36**, 2401315.
18 H. Zhua, M. Gu, X. Dai, et al, *Chem. Eng. J.*, 2024, **494**, 153235.
19 B. R. Li, P. F. Cao, T. Saito and A. Sokolov, *Chem. Rev.*, 2023, **123**, 701-735.
20 Q. Dong, T. Naren, L. Zhang, W. X. Jiang, M. M. Xue, X. Wang, L. B. Chen, C. S. Lee and Q. C. Zhang, *Angew. Chem. Int. Ed.*, 2024, **63**, e202405426.
21 J. Sokjorhor, C. Phantan, K. Ratanathawornkit and D. Crespy, *Adv. Funct. Mater.*, 2025, **35**, 2508274.
22 Y. Li, B. Jiang and Y. D. Huang, *Compos. Sci. Technol.*, 2022, **227**, 109564.
23 H. Wang, H. L. Ma, N. Gan, K. Qin, Z. C. Song, A. Q. Lv, K. Wang, W. P. Ye, X. K. Yao, C. F. Zhou, X. Wang, Z. X. Zhou, S. L. Yang, L. R. Yang, C. M. Bo, H. F. Shi, F. W. Huo, G. Q. Li, W. Huang and Z. F. An, *Nat. Commun.*, 2024, **15**, 2134.
24 F. L. Ma, B. Wu, S. W. Zhang, J. H. Jiang, J. H. Shi, Z. Y. Ding, Y. Zhang, H. Z. Tan, P. Alam, J. Lam, Y. Xiong, Z. Li, B. Z. Tang and Z. Zhao, *J. Am. Chem. Soc.*, 2025, **147**, 10803-10814.
25 Y. F. Zhang, Q. K. Sun, L. T. Yue, Y. G. Wang, S. W. Cui, H. C. Zhang, S. F. Xue and W. J. Yang, *Adv. Sci.*, 2022, **9**, 2103402.
26 Y. Zhu, Y. Guan, Y. F. Niu, P. Wang, R. J. Chen, Y. H. Wang, P. Wang and H. L. Xie, *Adv. Opt. Mater.*, 2021, **9**, 2100782.
27 W. M. Wan, D. Tian, Y. N. Jing, X. Y. Zhang, W. Wu, H. Ren and H. L. Bao, *Angew. Chem. Int. Ed.*, 2018, **57**, 15510-15516.
28 Y. Su, Y. F. Zhang, Z. H. Wang, W. C. Gao, P. Jia, D. Zhang, C. L. Yang, Y. B. Li and Y. L. Zhao, *Angew. Chem. Int. Ed.*, 2020, **59**, 9967-9971.
29 X. Y. Fang, Y. Q. Tang, Y. J. Ma, G. W. Xiao, P. Y. Li and D. P. Yan, *Sci. China Mater.*, 2023, **66**, 664-671.
30 Y. F. Zhang, W. Zhang, J. M. Xia, C. C. Xiong, G. C. Li, X. D. Li, P. Sun, J. B. Shi, B. Tong, Z. X. Cai and Y. P. Dong, *Angew. Chem. Int. Ed.*, 2023, **62**, e202314273.
31 W. F. Pu, D. J. Du, R. Liu, J. Y. Gu, K. W. Li, Y. Y. Zhang and P. G. Liu, *RSC Adv.*, 2016, **6**, 39522-39529.
32 M. L. Liu, Y. H. Xu, Y. Wang, X. Chen, X. Q. Ji, F. S. Niu, Z. Q. Song and J. Q. Liu, *Adv. Opt. Mater.*, 2017, **5**, 1600661.
33 R. Tian, S. M. Xu, Q. Xu and C. Lu, *Sci. Adv.*, 2020, **6**, eaaz6107.
34 Z. F. An, C. Zheng, Y. Tao, R. F. Chen, H. F. Shi, T. Chen, Z. X. Wang, H. H. Li, R. R. Deng, X. G. Liu and W. Huang, *Nat. Mater.*, 2015, **14**, 685-690.
35 N. Wang, J. Q. Li, Y. T. Ma, A. H. Xu, H. J. Tao, B. Y. Huang, S. Hao, J. J. Liao, S. W. Lin, Y. P. Tang, Y. Hou, C. Bian and X. G. Li, *J. Anal. Test.*, 2024, **8**, 493-504.
36 L. Largitte, N. A. Travlou, M. Florent, J. Secor and T. J. Bandosz, *J. Photoch. Photobio. A.*, 2021, **405**, 112903.
37 R. Tian, S. Gao, K. T. Li and C. Lu, *Nat. Commun.*, 2023, **14**, 4720.
38 W. Wei, M. H. Zhang, H. Yan, S. B. Nan, Z. X. Cong, Y. F. Dong and A. Tang, *J. Energy Chem.*, 2025, **102**, 703-711.
39 M. Q. Dai, B. Zhou and D. P. Yan, *Angew. Chem. Int. Ed.*, 2025, **64**, e202505322.
40 L. Zhou, J. M. Song, Z. Y. He, Y. W. Liu, P. Jiang, T. Li and X. Ma, *Angew. Chem. Int. Ed.*, 2024, **63**, e202403773.

View Article Online
DOI: 10.1039/D5SC09282E

The data supporting this article have been included as part of the Supplementary Information.